J. Physiol. (1981), **311**, *pp.* 161–178
With 10 *text-figures*
Printed in Great Britain

A STUDY OF PACE-MAKER POTENTIAL IN RABBIT SINO-ATRIAL NODE: MEASUREMENT OF POTASSIUM ACTIVITY UNDER VOLTAGE-CLAMP CONDITIONS

BY JAMES MAYLIE, MARTIN MORAD AND JAMES WEISS

From the Department of Physiology,
University of Pennsylvania School of Medicine,
Philadelphia, Pennsylvania 19104, U.S.A.

(*Received 30 January 1980*)

SUMMARY

1. A single sucrose-gap voltage-clamp technique was used to control the membrane potential and to measure current in rabbit sino-atrial (SA) strips. K^+ activity in the extracellular space was simultaneously measured using K^+-selective micro-electrodes.

2. Using double-barrelled K^+-selective micro-electrodes it was possible to measure the time course of accumulation or depletion of K^+ accompanying a single action potential without complications arising from mechanical or electrical artifacts.

3. K^+ activity in the extracellular space increased during the action potential and then decreased to base-line levels during the diastolic depolarization phase. Single beat accumulations of 0·1–0·4 M could be measured.

4. The magnitude of accumulation or depletion of K^+ depended upon the membrane potential such that K^+ accumulated at potentials positive to -50 mV (K^+ efflux greater than K^+ uptake) and was depleted from the extracellular space at potentials negative to -50 mV (K^+ efflux less than K^+ uptake).

5. The rate of K^+ depletion was fairly constant during the time course of a clamp step within the range of diastolic depolarization (-55 to -75 mV) even though the accompanying membrane current showed marked time-dependent kinetics.

6. The total membrane conductance measured during the time course of the diastolic depolarization or during the time course of activation of time-dependent 'pace-maker' current remained fairly constant or increased.

7. No reversal potential for the time-dependent 'pace-maker' current could be measured at E_K in solutions containing 2·7, 5·4 and 8·1 mM-K^+.

8. These results do not support the turn-off of a K^+ conductance as the primary mechanisms for the generation of the pace-maker potential in SA nodal tissue; rather the results are more consistent with the idea that activation of an inward current, with large positive equilibrium potential, is responsible for pace-making activity.

0022-3751/81/3190-0766 $07.50

INTRODUCTION

Extensive physiological and pharmacological experiments have been carried out to determine the ionic mechanism responsible for the generation of diastolic depolarization in Purkinje fibres (for review see Noble, 1975; Tsien & Carpenter, 1978). It is concluded generally that the ionic mechanism responsible for the generation of diastolic depolarization is the decrease in potassium conductance in the presence of a constant or slightly increasing inward sodium and/or calcium current. This conclusion is based primarily on two observations. First, the membrane slope conductance was found to decrease during diastolic depolarization (Weidmann, 1951). Secondly, a time-dependent inward current (Vassalle, 1966) with a reversal potential at E_K (Noble & Tsien, 1968; Peper & Trautwein, 1969) seems to dominate in the pace-maker potential range.

Voltage-clamp experiments in the sino-atrial (SA) tissue have only recently met with some success (Noma & Irisawa, 1976*a*, *b*; Seyama, 1976; Brown, Giles & Noble, 1976). Although there are general similarities between the Purkinje and SA nodal tissue, major differences have been found (Irisawa, 1978) which may be responsible for the electrophysiological differences reported earlier between the two types of pace-maker cells (Brooks & Lu, 1972).

In this report we have used the K^+-selective micro-electrode in conjunction with the voltage-clamp technique (Kline & Morad, 1976; Goldman & Morad, 1977*b*) to determine the role of K^+ current in generation of the diastolic depolarization in the rabbit sino-atrial node. The results show that the time-dependent changes in the membrane current in the pace-maker potential range do not primarily reflect changes in the K^+ permeability.

A preliminary report of these findings has been published (Weiss, Maylie & Morad, 1978; Maylie, Weiss & Morad, 1979).

METHODS

Preparation. Rabbits (1·5–2 kg) were sacrificed by a blow to the head. The right atrium and the terminal segments of vena cava were cut away from the rest of the heart and were pinned in a perfusion chamber. Strips (0·3–0·5 mm in diameter and 10 mm in length) were cut from the region of the sino-atrial node parallel to the crista terminalis. If these strips showed fairly regular autorhythmicity they were then placed in a modified single sucrose-gap voltage-clamp chamber (Morad & Orkand, 1971). The results described below were obtained only from those strips which showed spontaneous electrical activity for the duration of experimental period (2–5 hr). Tetrodotoxin (10^{-6} M) had little or no effect on the rate of diastolic depolarization of these preparations although the rate of upstroke of the action potential was often somewhat depressed.

Solutions. The solutions normally perfused in the three compartments had the following composition (mM). (*a*) Tyrode solution: NaCl 137, KCl 2·7–8·1; $CaCl_2$ 1·8; $MgCl_2$ 0·7; NaH_2PO_4 0·4; $NaHCO_3$ 12; glucose 11; pH 7·4 by continuous bubbling in 98 % O_2 and 2 % CO_2; (*b*) sucrose solution: sucrose 262 (special enzyme grade, Schwarz-Mann); $MnSO_4$ 0·01; (*c*) KCl-Tyrode: KCl 140; $MgCl_2$ 0·7; NaH_2PO_4 0·4; $NaHCO_3$ 12; pH adjusted to 7·4 by bubbling in 98 % O_2 and 2 % CO_2. The sucrose and KCl-Tyrode solutions were kept at room temperature. The temperature of the Tyrode solution entering the chamber was varied between 25 and 36 °C. In general a temperature of 30 °C was sufficient to maintain uniform spontaneous pacing. In some experiments tetrodotoxin (TTX, Sigma) was added to the normal Tyrode solution.

Instrumentation. A 'chopped current-pulse clamp' technique similar to that used by Goldman & Morad (1977*b*) was used to compensate for the extracellular series resistance throughout the

voltage-clamp step. The chopped current-pulse clamp alternated between two phases of operation, a potential measurement and a current application phase with a frequency of 0·5–4 kHz. During the potential measurement phase the membrane potential way sampled only when the applied current was turned off so that there was no *IR* drop across the extracellular series resistance. This potential was compared with the command potential and the resulting error signal was stored and fed back through the clamp loop during the current application phase. A current pulse proportional to the stored error signal was applied through the sucrose gap which charged the membrane capacitance in the direction which minimized the error signal. Thus the feed-back loop operated to hold the transmembrane potential constant. The duty cycle of the on and off phases was variable so that the sampling period of the membrane potential could be adjusted between the 0·8 and 0·3 part of the total cycle. This modification made it possible to increase the sampling time such that the time for equilibration of membrane potential between various electrical 'patches' of the preparation was improved during the voltage measuring phase. The signals were digitized and recorded on cassette tapes by a mini-computer system (Alpha-16, Computer Automation) similar to that described previously (Goldman & Morad, 1977*b*).

K^+-selective electrodes. Double-barrelled K^+-selective electrodes were prepared as described by Kline & Morad (1976 & 1978). One barrel filled with normal Tyrode solution was used as a reference barrel to measure the extracellular potential artifact. The second barrel filled with the K^+-selective resin measured both the K^+ activity and the extracellular potential artifact. The extracellular K^+ activity was obtained by subtracting the signal of the reference barrel from that of the K^+ barrel. The tip diameter of the electrode ranged between 2 and 4 μm.

Upon insertion of the K^+ electrode into the muscle the K^+ barrel showed a large positive deflexion and the reference barrel a typical intracellular action potential. As the electrode settled into a paracellular space the recorded K^+ activity decreased to within a few tenths of a millimole of the bath K^+ concentrations (2·7 mM) and the signal from the reference barrel decreased to a few millivolts in magnitude. K^+-selective electrodes once in place responded to changes in $[K^+]_o$ to the same extent that they did in the calibrating solutions. The measured K^+ signal in mV was converted to concentration units (mM) using a calibration curve from the response of the electrode to addition of various $[K^+]$ concentrations to the bath. Unless otherwise indicated the K^+ concentration scale in each figure is logarithmic.

Evaluation of SA nodal strips for voltage-clamp experiments. Since the experiments to be described in this paper were carried out on SA nodal strips it is important at this juncture to outline some of the criteria used by us in evaluating our preparation. In was required that: (1) SA nodal strips paced spontaneously when placed in the single sucrose gap chamber, (2) development of twitch tension be accompanied by the action potential, independent of the position of the micro-electrode impalement. Often strips showed electromechanical uncoupling. In such cases the time course of change in K^+ activity did not occur simultaneously with the action potential. Electromechanical uncoupling was seen more consistently in those preparations where the strips were cut perpendicular to the crista terminalis. Such findings suggested that even in preparations as small as 0·3 mm in diameter and 0·4 mm in length local electrical blocks may occur. In the experiments described below only those strips were used that showed no electromechanical uncoupling.

Since squeezing of the extracellular space during contractile activity may alter the profile of the K^+ accumulation, experiments were carried out in which developed tension was altered or completely suppressed. Large accumulations of K^+ in the extracellular space accompanied spontaneous beating despite complete suppression of twitch tension in Ca^{2+}-free solution. Twitch tension was also increased by overdriving spontaneously pacing strips, causing marked increase in base-line K^+ concentrations without any change in base-line tension. These results suggest that the recording of K^+ activity in the extracellular space of SA nodal preparations are not significantly affected by mechanical squeezing or shortening of the tissue. We feel that measurement of tension simultaneously with the action potential serves as a good indicator of the extent of electrical homogeniety in the SA nodal strips.

Strict criteria were used to evaluate the adequacy of the clamp technique in the SA node. The following conditions were satisfied before a preparation was considered acceptable. (1) Considering a space constant of 828 μm in SA nodal tissue (Seyama, 1976) the physiological node was kept to less than 400 μm in length. (2) The intracellular micro-electrode was placed half-way between the sucrose gap and the end of the muscle tied to the tension transducer (Goldman & Morad, 1977*a*). (3) The currents were required to be smooth with no transient current spikes or bumps. (4) The

transgap action potential was required to be of similar time course and at least 50% in amplitude compared with that recorded intracellularly. Longitudinal homogeniety was not examined with a second micro-electrode because it was checked directly by the micro-electrode used in the chopped current-pulse clamp technique which samples the membrane potential during the zero-current flow phase. Preparations that were not easily controlled showed transient spikes in the membrane potential and membrane current and were rejected.

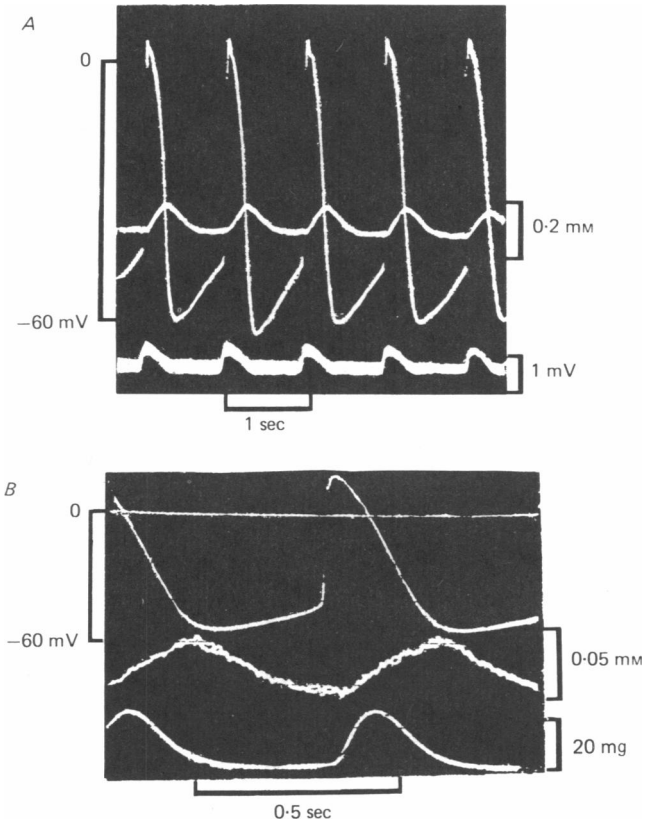

Fig. 1. Measurements of K^+ activity in the extracellular space in a whole sino-atrial preparation and a sino-atrial strip. In *A* single beat accumulations of extracellular K^+ (middle trace) are superimposed on the record of action potentials measured with an intracellular micro-electrode. The extracellular potential (bottom trace) measured from the reference barrel of the double-barrelled electrode was subtracted from the potential measured from the K^+ barrel to obtain the K^+ activity shown in the middle trace. *B* shows the time course of extracellular K^+ accumulation and depletion (middle trace) during spontaneous activity in an isolated rabbit SA nodal strip (diameter 0·5 mm, length 0·5 mm). Displayed on the top trace are action potentials recorded from an intracellular micro-electrode. Contractile activity is displayed on the bottom trace. $[K^+]_o = 2·7$ mM.

RESULTS

Experiments with K^+-selective electrodes

The time course of K^+ accumulation and depletion in SA nodal tissue. The time course of change in extracellular K^+ activity was measured both in whole SA nodal preparations and in spontaneously pacing strips isolated from the SA node. Fig. 1*A* shows simultaneous recordings of transmembrane electrical activity, the extracellular

potential changes and the extracellular K^+ activity in an autorhythmic whole sino-atrial preparation. Note that accumulation of K^+ occurred primarily during the time course of the action potential. During diastolic depolarization the K^+ activity returned back to the base-line level. The electrical signal obtained from the reference barrel of the K^+-electrode (Fig. 1*A*, lower trace) was subtracted from the signal obtained from the resin-containing barrel to obtain the changes in K^+ activity only (Fig. 1*A*, upper trace; see Kline & Morad, 1978). Fig. 1*B* shows a recording of the intracellular transmembrane potential, K^+ activity in the extracellular space and the

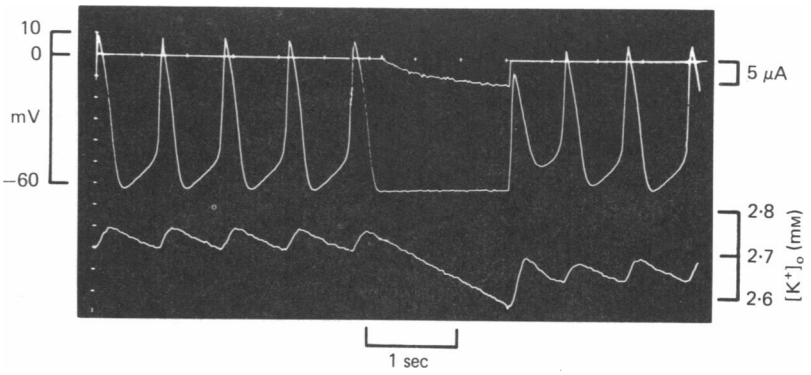

Fig. 2. Measurement of K^+ activity in voltage-clamped sino-atrial strip. A decrease in the activity of extracellular K^+ (bottom trace) is observed when spontaneous pace-making activity is interrupted at the maximum diastolic potential with a 1400 msec clamp step to −62 mV (middle trace). K^+ activity returns slowly back to base-line levels after the release of the clamp as the pace-making activity resumes. A time-dependent inward current (top trace) is measured during the clamp step. Temp. 31 °C. $[K^+]_o$ = 2·7 mM. Chopping frequency 1 kHz, and current injection duty cycle 0·5.

developed tension from an isolated SA nodal strip placed in the sucrose-gap chamber. Comparison of the time course of K^+ activity and the development of tension shows that activation of tension preceded significant accumulation of K^+ and tension relaxed before peak accumulation of K^+ occurred. Simultaneous recording of tension in all of SA nodal strips examined consistently showed that the time course of development of tension and the change in K^+ activity were not related.

K^+ accumulation and depletion in voltage-clamped SA nodal strips. Fig. 2 shows a self-pacing sino-atrial strip in which the extracellular K^+ activity was measured continuously. The rhythmic activity was interrupted during diastole by clamping the membrane potential to −62 mV for a duration of 1400 msec. A gradually increasing inward current (the pace-maker current) was necessary to hold the membrane potential constant. During the clamp step K^+ activity decreased at a constant rate from 2·73 to 2·58 mM. Upon termination of the clamp step spontaneous pacing resumed and the base-line K^+ activity returned gradually back to control levels. Consistent and fairly large depletions of K^+ from the extracellular space could be recorded depending on the duration and magnitude of the hyperpolarizing pulse.

The voltage dependence of the K^+ accumulation or depletion process was then examined in the auto-pacing strips. Clamping the membrane to potentials positive to about −50 mV consistently produced K^+ accumulations in the extracellular space,

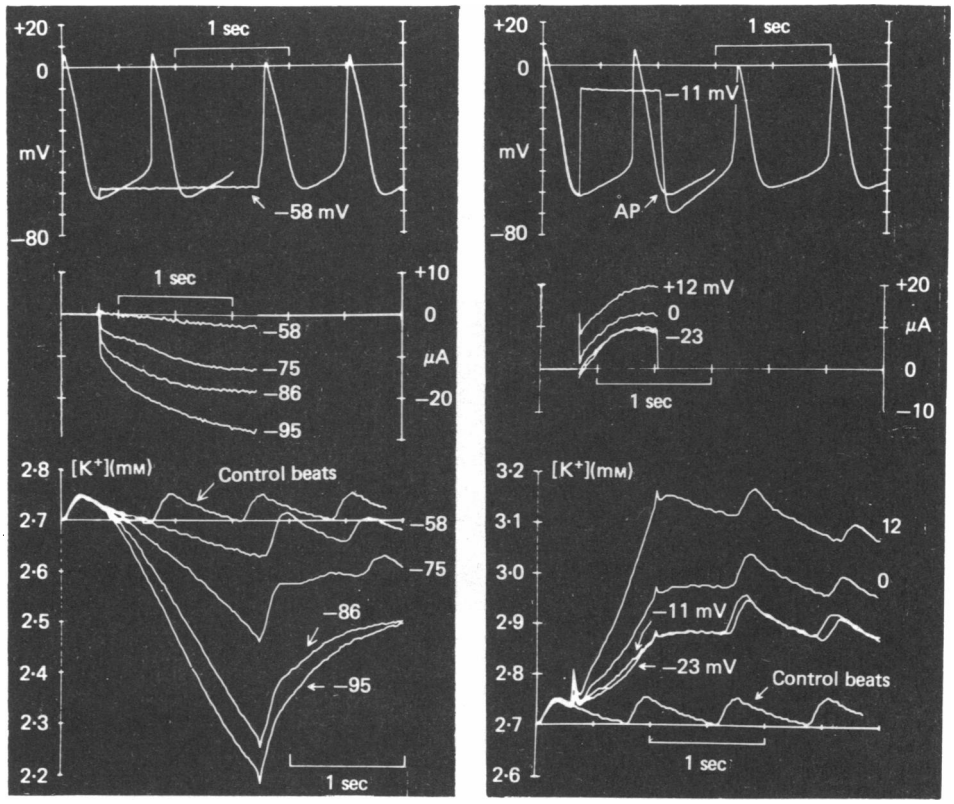

Fig. 3. Potential dependence of accumulation and depletion of K^+ in SA nodal strips. The left panels show superimposed measurements of K^+ depletion (bottom traces) in response to hyperpolarizing clamp steps initiated at the maximum diastolic potential (upper traces). The respective currents are superimposed on the middle traces and the clamp potentials are indicated beside each trace. K^+ accumulation during depolarizing clamp steps is shown in the right panels. The transient spikes in the K^+ activity at the beginning and end of each clamp step reflects the difference in response time to the electrical signal between the reference barrel (1 MΩ) and the K^+ barrel (100 MΩ). The data was replayed from digital tapes obtained by a mini-computer. The measured K^+ activity has been linearized using a procedure described in Methods. $[K^+]_o$ = 2·7 mM; temp. 31 °C. Chopping frequency 1 kHz; current injection duty cycle 0·5.

and these decayed slowly back to base-line activity following the clamp step. Hyperpolarizing pulses caused depletion of K^+ from the extracellular spaces. Fig. 3 shows superimposed traces of the membrane current and the change in extracellular K^+ activity resulting from voltage-clamp pulses initiated at the point of the maximum diastolic potential in an auto-pacing strip. Increasing clamp steps in the hyperpolarizing direction increased the magnitude and rate of K^+ depletion from the extracellular space (Fig. 3, left panel). The time-dependent current necessary to hold each clamp step constant became more inward and seemed to approach a steady-state value within 2 sec. Depolarizing clamp steps positive to −50 mV produced a transient inward current followed by a steady-state outward current (Fig. 3, right panel). The change in K^+ activity accompanying these pulses seemed to reflect

the rectification of the membrane current (compare traces for −11 and −23 mV in Fig. 3).

Rate of accumulation and depletion of K^+. In Fig. 3 the increasing inward pace-maker current was accompanied by depletion of K^+ from the extracellular space. Taken at face value this observation is consistent with the hypothesis that a decrease of K^+ conductance is responsible for the generation of the diastolic depolarization. Since the rate rather than the magnitude of accumulation or depletion of K^+ reflects the net flux of K^+ into the space (and therefore the conductance of membrane to K^+), a comparison of initial and final rates of accumulation or depletion accompanying

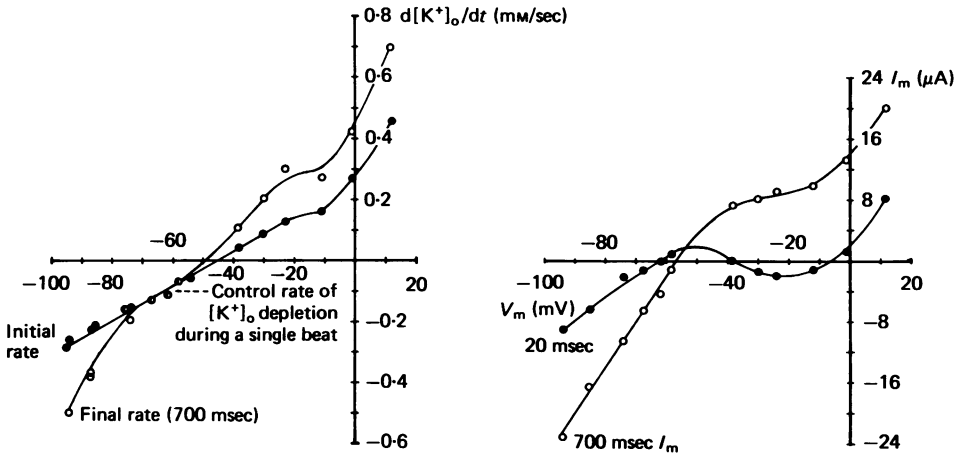

Fig. 4. Comparison of K^+ fluxes at the initiation and termination of clamp steps. Left graph: plot of the initial (filled circles) and final (open circles) rate of K^+ depletion or accumulation vs. the clamp potential. The initial rate of change of K^+ activity was measured at the beginning of the clamp step and the final rate 700 msec into the clamp step. The rate is expressed in mM/sec. Note that in the vicinity of pace-maker potential (−70 to −55 mV) the initial and final rates of K^+ depletion are the same. Right graph: plot of initial and final currents *vs.* the clamp potential. During hyperpolarizing pulses the initial current was taken as the peak outward-going current at the beginning of the clamp (20 msec) whereas for depolarizing clamps the initial current was taken as the peak transient inward current. Data points are obtained in part from original records shown in Fig. 3.

the clamp step was undertaken. Fig. 4 shows the plot of the initial and final rates of K^+ accumulation or depletion and the initial (20 msec) and final (700 msec) membrane currents at various clamp potentials. For clamp potentials more negative to −75 mV and positive to −55 mV the final rates were larger than the initial rates of accumulation or depletion. However, in the range of the diastolic potentials the initial and final rates of K^+ depletion were similar even though the membrane currents showed considerable time dependence (Figs. 3 and 4). These findings suggest that the time-dependent inward current associated with pace-making activity in the SA nodal cells may not be primarily due to the turn-off of the K^+ current.

Magnitude of K^+ accumulation in the SA nodal tissue. Since the tip of K^+-selective electrode was 2–4 μm, it is reasonable to assume that the placement of electrode in the preparation distorts and enlarges the extracellular space. Such enlargement of

the extracellular space would tend to dilute the transmembrane flux of K^+ in the vicinity of the electrode tip. An estimate of the dilution factor was obtained by comparing the response of the K^+ electrode following a clamp-induced accumulation of K^+ with that simultaneously detected by the membrane potential. The selectivity of the electrode to K^+ in the extracellular space of the muscle was measured by altering bath concentrations of K^+, and was found to be the same (50:1 for K:Na) as that measured in bath calibrating solutions (see also Kline & Morad, 1976, 1978). The selectivity of SA nodal membrane to K^+ was found to be 22 mV per decade change

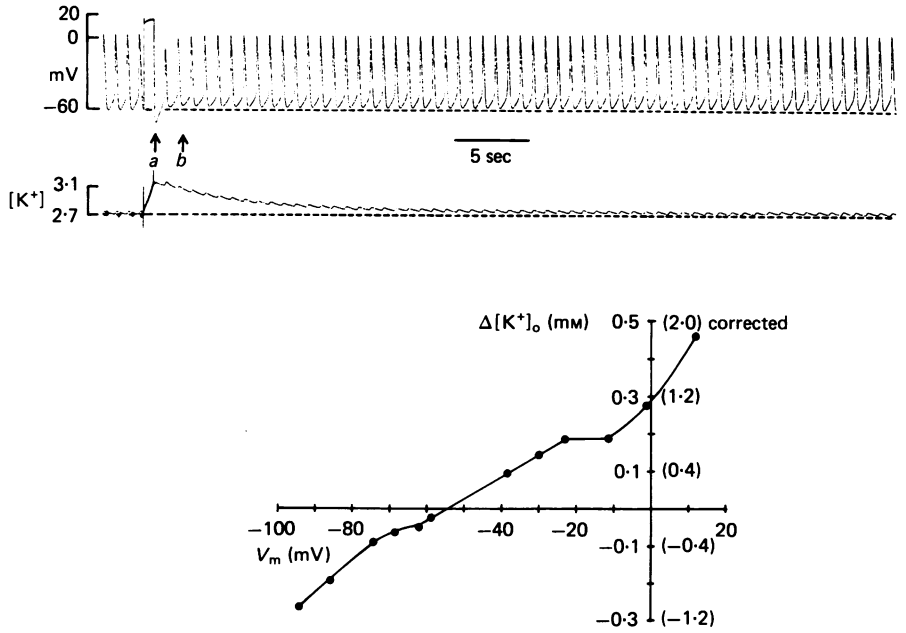

Fig. 5. Estimation of the dilution factor around the tip of the K^+ electrode in SA nodal strip. The chart recordings show recovery of the maximum diastolic potential (top trace) and K^+ activity (second trace) following a depolarizing clamp step to +14 mV. Point *a* marks the first maximum diastolic potential following the clamp and point *b* marks the location used to calculate the dilution factor. Plotted below the tracings is the total change in K^+ activity measured 700 msec into the clamp *vs.* the clamp potential. The values in parentheses are the corrected changes in K^+ activity as determined by the estimated dilution factor. The data points were obtained from the same experiment as that illustrated in Fig. 3.

of $[K]_o$, a value similar to that found previously (DeMello, 1961; Irisawa, 1978). Fig. 5 (upper panel) compares the response of the K^+ electrode and membrane potential following a clamp step to +15 mV. After the initial post-clamp hyperpolarization (point a), subsequent maximum diastolic potentials remained at more depolarized values (point b) and returned to the control values with the same time course (half-time 5–10 sec) as that of the extracellular K^+ activity (lower trace). The change in maximum diastolic potential above the base-line (ΔV) was an indicator of the average change in the extracellular K^+ activity. $\Delta[K^+]$ was calculated using a modification of the Nernst equation ($\Delta[K^+] = [K^+]_o\ (10^{\Delta V/22} - 1)$; see also Cleemann & Morad, 1979). For $[K^+]_o$ of 2·7 mM and a ΔV of 4 mV (from −61 to −57 mV) a value of 1·4 mM

for $\Delta[K^+]$ was obtained. Since the accumulation of K^+ measured by the K^+ electrode was 0·36 mM (measured at point *b*, Fig. 5), it seems as if the K^+ activity was diluted by a factor of 4 in the space created by the electrode tip. The measured change in K^+ activity was on the average 25 % ± 5 ($n = 6$) of that predicted from using the membrane potential as a sensor of K^+ activity. The graph of Fig. 5 shows the voltage dependence of accumulation and depletion of K^+ activity in the extracellular space measured following a 700 msec clamp pulse. The scale on the left of the ordinate reflects the K^+ activity measurements obtained from the K^+ electrode and the scale on the right depicts the measurements of K^+ activity based on the selectivity of the maximum diastolic potential to K^+. These results indicate that fairly large changes in K^+ activity may be produced during spontaneous pacing or under voltage-clamp conditions in SA nodal tissue. Although significant changes in E_K may recur with clamp steps of long duration, changes in E_K with short clamps in the range of pacemaker potentials seem to be insignificant.

Terminations of depolarizing voltage-clamp steps (in the range −40 to +20 mV) were usually followed by hyperpolarizing after-potentials for a single beat (e.g. Fig. 5, upper trace). Although activation of a K^+ conductance in this potential range may be responsible for such a hyperpolarization, alternate possibilities such as activation of an electrogenic pump or inactivation of an inward current may also contribute to such a hyperpolarizing maximum diastolic potential. Preliminary experiments showed that these hyperpolarizing post-clamp potentials were markedly suppressed in the presence of low Cl^- solutions but not in ouabain or low Ca^{2+} and low Na^+ solutions. Consistent with this assertion was the finding that following clamp steps to −30 or up to 0 mV (Fig. 3), the activity of K^+ does not change during diastole following the clamp step despite marked enhancement in the rate of diastolic depolarization.

Voltage-clamp studies

As indicated earlier, the two major experimental findings which support the turn-off of the K^+ conductance in generating the pace-making activity in Purkinje fibres are: (1) a decrease of membrane conductance during diastolic depolarization (Weidmann, 1951) and (2) a reversal potential for the inward current associated with pace-making at E_K (Noble & Tsien, 1968). These two findings are not fully substantiated in the SA nodal cells (Irisawa, 1978). Since the results obtained from K^+-electrode experiments do not support the K^+ hypothesis, in the experiments described below we re-investigated the time course of conductance change during diastolic depolarization and determined whether the pace-maker current reverses at E_K.

Measurements of total membrane conductance during diastolic depolarization. Fig. 6 shows original tracings from an experiment in which small clamp pulses were applied at various times during the diastolic depolarization. The 5 msec current–voltage relation (see Goldman & Morad, 1977*b* for criteria) were measured at three different times during the pace-maker potential. The plot of the 5 msec I–V relation indicates that during diastolic depolarization membrane conductance increased slightly or remained fairly constant. In this experiment the total membrane capacitance was 0·5 μF, giving a total conductance of 150 μmho/μF at the point of maximum diastolic potential. The measurement of membrane conductance at 5–10 msec into the test pulse consistently showed that the total membrane conductance increased during the time course of the diastolic depolarization in ten preparations tested (Table 1). The conductances were measured with small pulse voltage perturbation in the

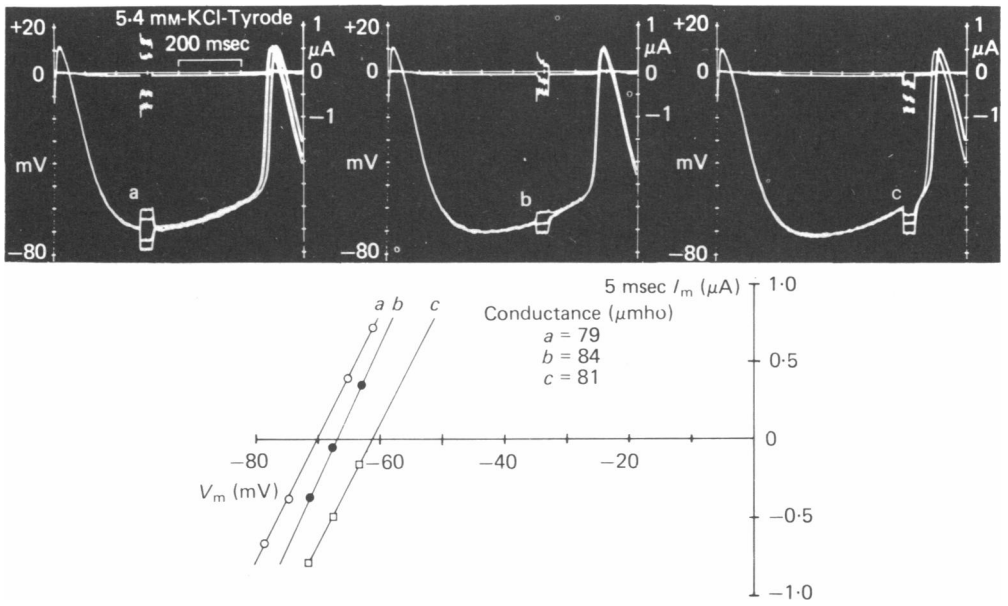

Fig. 6. Measurement of total membrane conductance at three different times during diastolic depolarization. Upper panels show records of the membrane current (top trace) in response to small pulse voltage perturbation (40 msec in duration) about the pace-maker potential (lower trace). Plotted are the initial currents measured 5 msec following initiation of the clamp as a function of the clamped potential. The slopes of the 5 msec *I–V* curves determine the total membrane conductances as indicated. Note that the membrane conductance indicated in the inset of graph increases slightly during the diastolic depolarization. The data were replayed from digital tapes. Temp. 31 °C; $[K^+]_o$ = 5·4 mM; strip diameter 0·33 mm, length 0·4 mm; chopping rate 2 kHz; current injection duty cycle 0·2; total capacitance of preparation 0·5 μF.

TABLE 1. Total membrane conductance (μmho/μF)

Experiment	$[K^+]_o$ (mM)	M.d.p.	Midway between m.d.p. and e.d.p.	E.d.p.
22.5.78.	2·7	121	—	128
14.6.78.	2·7	316	—	321
30.8.78.	2·7	92	130	112
19.9.78.	2·7	246	281	275
2.10.78.	2·7	189	200	204
6.11.78.	5·4	134	165	140
9.11.78.	5·4	146	164	172
24.1.79.	5·4	140	143	150
25.1.79.	5·4	77	88	111
26.1.79.	5·4	158	168	162

The total membrane conductance was measured at 5 msec into the pulse at maximum diastolic potential (m.d.p.) and at mid point between the m.d.p. and end diastolic potential (e.d.p.) and about 20 msec before e.d.p. (see Fig. 6). The average period between m.d.p. and e.d.p. was about 400 msec.

range of diastolic depolarization where the initial I–V relation was fairly linear (see Fig. 4). Measurement of the membrane current at the end of the 40 msec pulses (a duration similar to that used in Purkinje fibres, Weidmann, 1951) at the three indicated times in Fig. 6 showed a decreasing membrane conductance during the diastolic depolarization phase (from 86 to 71 μmho). Such measurements were not considered as accurate indicators of total membrane conductance since considerable time-dependent current developed at the end of a 40 msec clamp step.

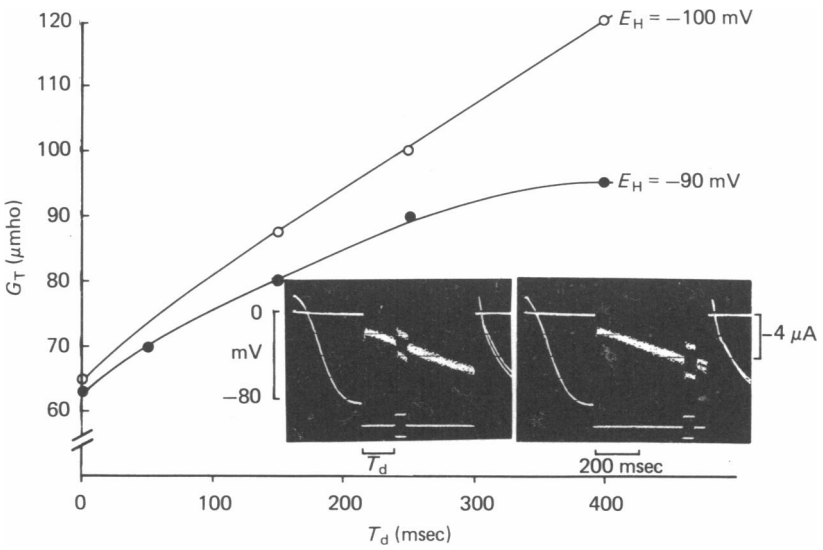

Fig. 7. Measurement of total membrane conductance during the 'pacemaker' current. Plotted is the total membrane conductance measured at different times during activation of time-dependent inward current at two holding potentials (−90 and −100 mV). The inset shows two records from the same experiment, demonstrating the small pulse voltage perturbation technique used to measure the total membrane conductance. The conductance at each time was calculated from the 5 msec I–V curves. Note that conductance increases during the activation of the time-dependent inward current. Temp. 30 °C; $[K^+]_o$ = 2·7 mM; chopping frequency 2 kHz; current injected duty cycle 0·2, strip diameter 0·35 mm, length 0·4 mm.

The total membrane conductance was also measured during the time course of the inward pace-maker current. Fig. 7 shows that total membrane conductance increased within the time course of activation of the pace-maker current. The increase in conductance was also seen at more negative potentials where the pacemaker current was more strongly activated (Fig. 3).

Since the total membrane conductance increased only slightly during the diastolic depolarizations, it is reasonable to assume that the sum of the inward and outward ionic conductances are closely balanced during the time course of the pace-maker potential. Since E_{Na} and E_{Ca} are much larger than E_K with respect to the maximum diastolic potential, such a balance of conductances would tend to favour a larger contribution from Ca^{2+} and/or Na^+ flux than K^+ fluxes across the membrane during diastolic depolarization.

Reversal potential for pace-maker current. In the experiments illustrated below an attempt was made to determine whether a reversal potential for the inward pace-making current could be found which would be equivalent to the calculated E_K. Thus, the time course of the pace-maker current and its potential dependence were studied at various external K^+ concentrations (2·7, 5·4 and 8·1 mM). The K^+ equilibrium potential for such K^+ concentrations have been previously determined for the rabbit SA node (−102, −85, −76 mV, respectively; DeMello, 1961). Fig. 8 shows that even in 8·1 mM $[K^+]_o$ the time-dependent inward currents did not reverse

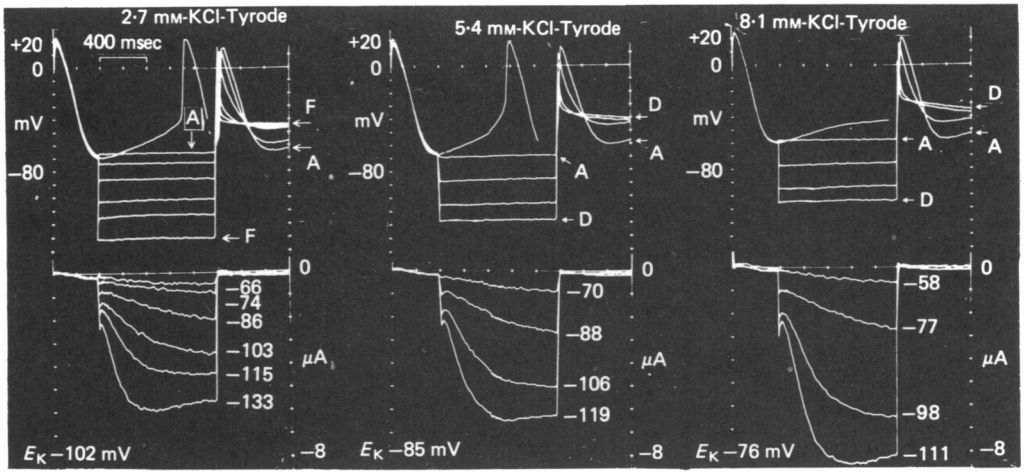

Fig. 8. Potential dependence of pace-maker current in three K^+ concentrations (2·7, 5·4 and 8·1 mM). Each record shows superimposed traces of the membrane potential (top) and current (bottom). The calculated K^+ equilibrium potential for each K^+ concentration, indicated in the lower left corner of each record, is −102 mV, −85 mV and −76 mV, respectively. Note that the time-dependent inward pace-maker current does not show any indication of reversing in direction at the potentials indicated. Data were replayed from digital tapes. Temp. 27 °C; chopping frequency 1 kHz; current injection duty cycle 0·5; total capacitance of strip 0·6 μF.

for clamp steps up to −111 mV (35 mV negative to the expected E_K). The expected reversal potentials for the various solutions are indicated in the bottom left corner of each panel. The time-dependent inward current does not show any indication of reversal in direction, and was more strongly activated for increasing hyperpolarizing steps.

The difference between the final and the initial current (i.e. the time-dependent inward current associated with pace-making) was plotted as a function of the clamp potential (Fig. 9). The plot of the time-dependent current ΔI_m represents the degree of activation or inactivation of a specific current and should have crossed the zero-current axis at clamped potentials equal to E_K (reversal potential) had the current been due to inactivation of K^+ conductance. The I–V relation for ΔI_m at each $[K^+]_o$ showed no indication of approaching the zero I_m axis. In fact, the time-dependent inward currents were accentuated by increasing the $[K^+]_o$. The lack of a true reversal potential for the time-dependent inward currents around E_K further argues against

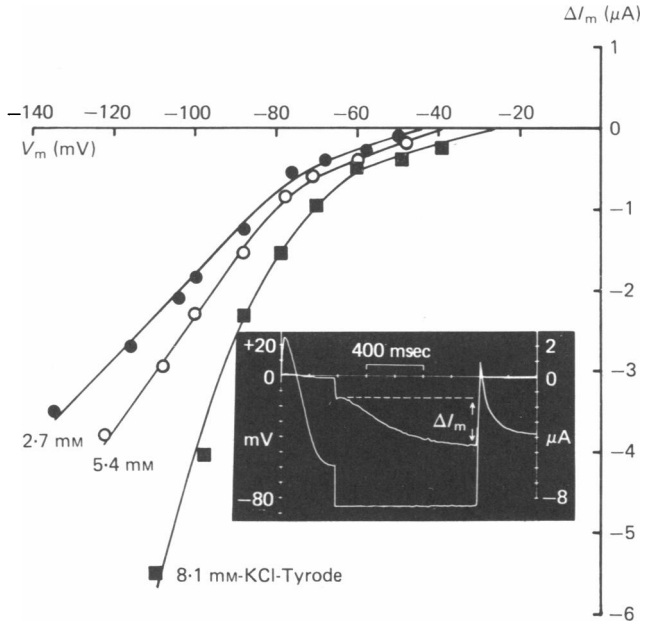

Fig. 9. Plot of the change in the time-dependent inward current (ΔI_m) as a function of the clamp potential in 2·7, 5·4 and 8·1 mM-KCl-Tyrode solution ΔI_m was obtained as the difference between the final and the initial membrane current (see inset). Data points are obtained from the same experiment as that illustrated in Fig. 8.

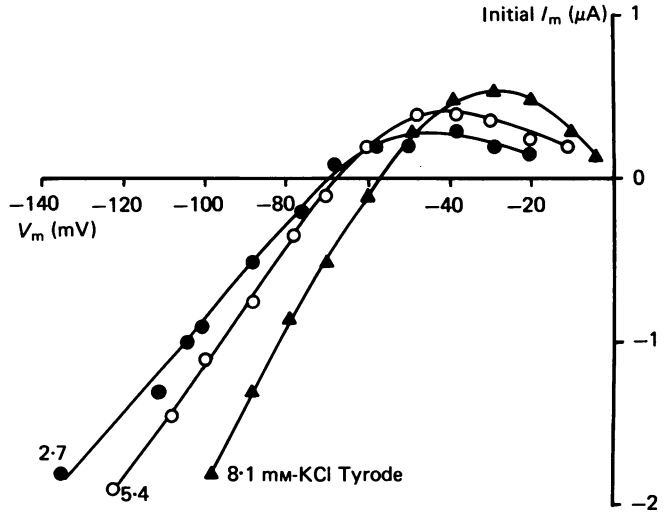

Fig. 10. K^+ dependence of the initial membrane current in the SA node. Plotted are the current–voltage relations for the initial membrane current in the three indicated K^+ concentrations, 2·7 (closed circles), 5·4 (open circles) and 8·1 mM (closed triangles). The initial membrane current (10 msec into the clamp step) was measured following the capacitive surge and before any time-dependent changes in membrane current occurred. Increasing the K^+ concentration shifted the I–V relation toward more positive potentials and increased the maximum outward current. Data were obtained from the experiment in Fig. 8.

a primary role for the turn-off of K^+ conductance in determining the pace-maker potential.

K^+ dependence of initial membrane current. The initial membrane current was plotted in Fig. 10 as a function of the membrane potential for the three K^+ concentrations indicated. The *I–V* relations show the characteristic inward rectification that has been described in Purkinje fibres (Noble & Tsien, 1968) and in frog ventricle (Cleemann & Morad, 1979). Increasing the $[K]_o$ shifted the *I–V* relations along the membrane potential axis towards more positive potentials and increased the maximum outward current. The *I–V* relation for each K^+ concentration was practically linear for hyperpolarizing pulses. The slope conductance, measured at the intercept of the voltage axis increased with increasing K^+ concentrations. Measurement of membrane conductance (using small pulse perturbations) at the maximum diastolic potential also showed an increase in membrane conductance when $[K^+]_o$ was increased from 2·7 to 8·1 mM. These findings suggest that the pace-maker membrane becomes more selective to K^+ with increasing $[K^+]_o$ which in turn may result in a decreased rate of diastolic depolarization (Fig. 8).

DISCUSSION

The major findings of this study are that in SA nodal strips the total membrane conductance increases slightly during the time course of the diastolic depolarization or during the generation of the inward pace-maker current. No reversal potential for the pace-maker current could be found when the membrane potential was clamped to a series of potentials in the range of expected E_K. Simultaneous application of the voltage clamp and K^+-electrode techniques showed that fairly large accumulation or depletion of K^+ did occur in the extracellular space, but that the rate of depletion or accumulation (a measure of net transmembrane flux of K^+) did not vary during the time course of a clamp step in the range of the pace-maker potential. These findings do not support the turn-off of a K^+ conductance system as the primary mechanism for the generation of the diastolic depolarization in the SA nodal tissue.

Voltage-clamp experiments in the SA nodal tissue. Considerable data regarding pacemaker activity have been obtained recently using the sucrose-gap and the two-micro-electrode voltage-clamp techniques (Brown *et al.* 1976; Noma & Irisawa, 1976*a*, *b*; Seyama, 1976; Irisawa, 1978). The voltage-clamp experiments in this report were performed in a modified single sucrose-gap arrangement in which the membrane potential that was applied to the feed-back amplifier was measured with intracellular micro-electrodes. In this respect the problems associated with the measurement of attenuated action potentials across a second sucrose gap due to transgap leakage currents were avoided (Irisawa, 1972; Brown *et al.* 1976). Furthermore in the chopped-current-pulse voltage-clamp technique, since the membrane potential is measured only in the zero-current phase of the feed-back cycle, the micro-electrode serves as a continuous check on the homogeniety of voltage distribution in the preparation (see Methods and Goldman & Morad, 1977*b*). Crucial to achieving adequate spatial control is that the space constant be longer than the length of the electrically active tissue. The average length of the tissue in our single sucrose-gap chamber was 400 μm. For an average length constant of 828 μm in SA nodal tissue

(Seyama, 1976), homogenous voltage control could be achieved within an error of 11 % for a terminated cable (Goldman & Morad, 1977*a*).

Inherent to the application of voltage-clamp techniques to multicellular tissue is the presence of a fairly large extracellular resistance which was found to be about 10–25 % of the total membrane resistance in SA nodal strips. By using a discontinuous current–pulse train in the feed-back loop we were able to functionally eliminate the *IR* drop across the extracellular resistance (Goldman & Morad, 1977*b*). The application of this technique improved the charging time of the membrane capacitance which made it possible to measure the membrane current 2–5 msec into the clamp, long before activation of the time-dependent pace-maker currents.

Evaluation of K^+ activity measurements. The clamp-induced changes of the K^+ activity in the extracellular space, as monitored by the K^+-selective micro-electrode, were transient with a re-equilibration half-time ranging between 5 and 10 sec. To assess the dilution factor induced by the electrode space, the K^+ activity following depolarizing clamp steps was compared with values predicted from the application of the Nernst equation to changes of the post-clamp membrane potential (see Cleemann & Morad, 1979 for validity of such comparison). Such a comparison in the SA node showed that the measured change of K^+ activity underestimates that indicated by the membrane potential by 75 % (a dilution factor of 4). Thus the results suggest that the double barrelled K^+ electrodes (with tip diameter of 2–4 μm) create an enlarged space around the electrode tip which in turn tend to dilute the transient changes of the transmembrane fluxes of K^+ by a factor of 4.

During the first 100 msec of the clamp steps the magnitude of accumulation or depletion of K^+ in the extracellular space (even when corrected for a dilution factor of 4) was not greater than 0·2 mM for the largest clamp steps (+10 mV or −95 mV). Thus it may be safely assumed that during short clamp pulses (50–100 msec) the time-dependent changes in membrane current are not significantly altered by small changes in E_K (Cohen, Daut & Noble, 1976). However, the change of K^+ activity in the extracellular space during the time course of longer clamp steps to +10 mV and −95 mV are sufficiently large (1·8 mM and −1·6 mM, respectively) as to cause large changes in E_K and alter the time-dependent currents (Baumgarten & Isenberg, 1977). Furthermore, as shown in Fig. 10, changes in the extracellular activity of K^+ will affect the inward rectification of K^+, causing both a change in permeability of the membrane to K^+ and a shift of I–V relations (Noble & Tsien, 1968; Cleemann & Morad, 1979).

Whether K^+ in the extracellular space accumulates or is depleted depends on the difference between the transmembrane efflux and influx of K^+. A measure of the net flux of K^+ can be obtained from measurements of the slope of the K^+ activity trace accompanying a clamp step. Thus if the magnitude of K^+ depletion accompanying the clamp step is small (i.e. E_K remains fairly constant), and active uptake or passive diffusion to bulk solution remain unchanged, then time-dependent changes in the K^+ conductance may be reflected by changes in the slope of K^+-depletion trace. Thus the finding that K^+ depletion during each individual clamp pulse in the pace-maker range was constant even though the membrane current showed considerable time dependence (Figs. 2 and 5) suggests that changes in the K^+ conductance were quite small.

Conductance measurements during the diastolic depolarization. Detailed measurements of membrane conductance during the time course of the diastolic depolarization show that the membrane conductance increased slightly or remained fairly constant in ten preparations (Fig. 6 and Table 1). A fairly large increase in membrane conductance was also seen during the development of the time-dependent pace-maker current (Fig. 7). These results are consistent with other conductance measurements in this tissue (Seyama, 1976) but contrast with those measured in Purkinje fibres by Weidmann (1951) and Vassalle (1966) who found a decrease in membrane conductance during diastolic depolarization and during the pace-maker current. However, such measurements in Purkinje fibres were generally made with longer pulses (50 msec) when time-dependent currents may have been activated. In fact, measurements of membrane conductance with 40 msec pulses in our preparations also yielded a decreasing membrane conductance during the time course of diastolic depolarization.

Calculations of the expected changes in the total membrane conductance during the time course of diastolic depolarization were based on equations similar to those used by Goldman & Morad (1977*c*) to separate the ionic conductances for a simplified model where only the Na^+ or K^+ conductance was allowed to change. Such calculations showed that the total membrane conductance would *decrease* by 25% when only the K^+ conductance was allowed to decrease during a diastolic depolarization potential of 10 mV at the rate of 50 mV/sec ($E_K = -86$ mV). On the other hand, an *increase* of only 10% in total membrane conductance would be required to produce the same diastolic depolarization if only the Na^+ conductance was allowed to increase ($E_{Na} = +40$ mV). Even much smaller changes in conductance are required if Ca^{2+} conductance with $E_{Ca} = +120$ mV is considered. Clearly, the conductance measurements in this study did not show a 25% decrease in membrane conductance but in fact showed a consistent but small increase (2–10%, Table 1). The results thus seem to be more consistent with activation of Na^+ or Ca^{2+} conductance during the diastolic depolarization.

An electrogenic Na^+–K^+ pump may also contribute to the development of diastolic depolarization (Isenberg & Trautwein, 1974; Irisawa, 1978; Eisner & Lederer, 1979). In this respect the pump may be modelled as a constant outward-current device with infinite impedence. Inactivation of the Na^+–K^+ pump during diastolic depolarization as a result of K^+ depletion from the extracellular space (Fig. 1*B*) would induce a time-dependent decreasing outward current. Such a process would result in membrane depolarization without detectable changes in the membrane conductance.

The reversal of time-dependent pace-maker current. Another major piece of evidence in support of the turn-off of K^+ conductance in generating the pace-maker activity is the finding that the 'pace-maker current' reverses at estimated E_K. We failed to observe a distinct reversal potential for the time-dependent currents associated with pace-maker activity. In fact, the 'pace-maker current' seemed to activate even more strongly with larger hyperpolarizations (Fig. 9). Variations in $[K^+]_o$ from 2·7 to 8·1 mM also failed to show a reversal potential (up to -160 mV tested; a potential much larger than the E_K measured in this tissue, DeMello, 1961). Absence of a distinct reversal potential in the SA nodal tissue can also be seen, in part, in the records of Noma & Irisawa (1976*b*). These authors claim to have measured a reversal potential when $[K^+]_o$ was increased to 25–50 mM. However, at these K^+ concentrations pace-making activity is suppressed.

The absence of a reversal potential in our studies contrasts sharply with the results obtained to date in either Purkinje or SA nodal preparations. Although no conditioning clamp steps were used in our studies, compared to those of Irisawa and co-workers, no obvious reason seems to exist for the difference between the two sets of data. It is conceivable, however, that the apparent 'reversal potential' is caused by depletion-induced time-dependent K^+ currents, similar to those described by Cleemann & Morad (1979) in ventricular tissue. According to such a possibility, the depletion-induced currents (inwardly decreasing), may be sufficiently large to mask the true time-dependent pace-maker currents (which are inwardly increasing). The extent to which the two currents dominated at a given clamp step would thus determine the direction of the net membrane current. In fact, if the membrane potential was clamped negative to maximum diastolic potential by 60 mV or more we often observed indications of depletion-induced currents superimposed on the time-dependent pace-maker current (Fig. 8, $[K^+]_o$ 2·7 mM). Such depletion currents seemed to appear at less negative potential when $[K^+]_o$ was increased (compare 2·7, 5·4 and 8·1 mM in Fig. 8). In experiments of Irisawa and co-workers where $[K]_o$ had been increased to 25–50 mM, it is conceivable that large voltage deflexions (60 mM or larger, from holding potentials of 0 mV), necessary to show reversal in fact may have reflected large depletion-induced K^+ currents that masked the much smaller time-dependent inward pace-maker current.

Considering the variations in clamp procedures, the extent of accumulation and depletion of K^+, the variations in tissue geometry and various external K^+ concentrations used to date by different investigators, it is not surprising that qualitative differences exist between the results obtained in different laboratories.

This work was supported by NIH grants HL 16152 and HL 05636.

REFERENCES

BAUMGARTEN, C. M. & ISENBERG, G. (1977). Depletion and accumulation of potassium in the extracellular clefts of cardiac Purkinje fibers during voltage clamp hyperpolarization and depolarization. *Pflügers Arch.* **368**, 19–31.

BROOKS, C. McC. & LU, H-H. (1972). *The Sinoatrial Pacemaker of the Heart*. Springfield: Charles C. Thomas.

BROWN, H. F., GILES, W. & NOBLE, S. J. (1976). Voltage clamp of frog sinus venosus. *J. Physiol.* **258**, 78–79*P*.

CLEEMANN, L. & MORAD, M. (1979). Extracellular potassium accumulation in voltage-clamped frog ventricular muscle. *J. Physiol.* **286**, 83–111.

COHEN, I., DAUT, J. & NOBLE, D. (1976). The effects of potassium and temperature on the pacemaker current, i_{K_2}, in Purkinje fibres. *J. Physiol.* **260**, 55–74.

DEMELLO, W. C. (1961). Some aspects of the interrelationship between ions and electrical activity in specialized tissue of the heart. In *The Specialized Tissues of the Heart*, ed. DeCarvalho, A. P., DeMello, W. C. and Hoffman, B: F. New York: Elsevier.

EISNER, D. A. & LEDERER, W. J. (1979). The role of the sodium pump in the effects of potassium-depleted solutions on mammalian cardiac muscle. *J. Physiol.* **294**, 279–301.

GOLDMAN, Y. & MORAD, M. (1977*a*). Regenerative repolarization of the frog ventricular action potential: a time and voltage-dependent phenomenon. *J. Physiol.* **268**, 575–611.

GOLDMAN, Y. & MORAD, M. (1977*b*). Measurement of transmembrane potential and current in cardiac muscle: a new voltage clamp method. *J. Physiol.* **268**, 613–654.

GOLDMAN, Y. & MORAD, M. (1977*c*). Ionic membrane conductance during the time course of the cardiac action potential. *J. Physiol.* **268**, 655–695.

IRISAWA, H. (1972). Electrical activity of rabbit sino-atrial node as studied by double sucrose gap method. In *Proc. Satellite Symp. 25th int. Congr. Europ. Brussels*, pp. 242–248. Presses Académiques Européenes.

IRISAWA, H. (1978). Comparative physiology of the cardiac pacemaker mechanism. *Physiol. Rev.* **58**, 461–498.

ISENBERG, G. & TRAUTWEIN, W. (1974). The effects of dihydro-ouabain and lithium ions on the outward current in cardiac Purkinje fibres. *Pflügers Arch.* **350**, 41–54.

KLINE, R. & MORAD, M. (1976). Potassium efflux and accumulation in heart muscle. *Biophys. J.* **16**, 367–372.

KLINE, R. P. & MORAD, M. (1978). Potassium efflux in heart muscle during activity: extracellular accumulation and its implication. *J. Physiol.* **280**, 537–558.

MAYLIE, J., WEISS, J. & MORAD, M. (1979). Pacemaker currents and extracellular K^+ activity in rabbit SA node. *Biophys. J.* **25**, 199*a*.

MORAD, M. & ORKAND, R. K. (1971). Excitation–contraction coupling in frog ventricle: evidence from voltage clamp studies. *J. Physiol.* **219**, 167–189.

NOBLE, D. (1975). *The Initiation of the Heartbeat*. Oxford: Clarendon Press.

NOBLE, D. & TSIEN, R. W. (1968). The kinetics and rectifier properties of the slow potassium current in cardiac Purkinje fibres. *J. Physiol.* **195**, 185–214.

NOMA, A. & IRISAWA, H. (1976*a*). Membrane currents in the rabbit sinoatrial node cell as studied by the double microelectrode method. *Pflügers Arch.* **364**, 45–52.

NOMA, A. & IRISAWA, H. (1976*b*). A time and voltage dependent potassium current in the rabbit sinoatrial node cell. *Pflügers Arch.* **366**, 251–258.

PEPER, K. & TRAUTWEIN, W. (1969). A note on the pacemaker current in Purkinje fibres. *Pflügers Arch.* **309**, 356–361.

SEYAMA, I. (1976). Characterstics of the rectifying properties of the sino-atrial node cell of the rabbit. *J. Physiol.* **255**, 379–397.

TSIEN, R. W. & CARPENTER, D. O. (1978). Ionic mechanisms of pacemaker activity in cardiac Purkinje fibres. *Fedn Proc.* **37**, 2127–2131.

VASSALLE, M. (1966). Analysis of cardiac pacemaker potential using 'voltage clamp' technique. *Am. J. Physiol.* **210**, 1335–1341.

WEIDMANN, S. (1951). Effect of current flow on the membrane potential of cardiac muscle. *J. Physiol.* **115**, 227–236.

WEISS, J., MAYLIE, J. & MORAD, M. (1978). Pacemaker currents and paracellular K^+ accumulation in rabbit sinoatrial node. In *Frontiers of Biological Energetics*, ed. Scarpa, A., pp. 1417–1426. New York: Academic Press.